FTIR and SEM Analysis of Polyester- and Epoxy-Based Composites Manufactured by VARTM Process

Volkan Cecen,[1] Yoldaş Seki,[2] Mehmet Sarikanat,[3] Ismail H. Tavman[1]

[1]*Department of Mechanical Engineering, Dokuz Eylul University, 35100 Bornova, Izmir, Turkey*
[2]*Department of Chemistry, Dokuz Eylül University, 35160 Buca, Izmir, Turkey*
[3]*Department of Mechanical Engineering, Ege University, 35100 Bornova, Izmir, Turkey*

Received 18 August 2006; accepted 26 November 2007
DOI 10.1002/app.27857
Published online 5 February 2008 in Wiley InterScience (www.interscience.wiley.com).

ABSTRACT: Polyester- and epoxy-based composites containing glass and carbon fibers were manufactured using a vacuum-assisted resin transfer molding (VARTM) process. Fourier transform infrared (FTIR) spectroscopy analyses were conducted to determine the interaction between fibers and matrix material. The results indicate that strong interaction was observed between carbon fiber and epoxy resin. However, weak interactions between remaining fiber-matrix occur. Scanning electron microscopy (SEM) analysis was also performed to take some information about strength of interaction between fibers and matrix material. From SEM micrographs, it is concluded that the findings in SEM analysis support to that obtained in FTIR analysis. Another aim of the present work was to investigate the influence of matrix on composite properties. Hence, the strengths of composites having same reinforcement but different matrix systems in axial tension and transverse tension were compared. Short beam shear test has been conducted to characterize the interfacial strength in the composites. © 2008 Wiley Periodicals, Inc. J Appl Polym Sci 108: 2163–2170, 2008

Key words: carbon fiber; glass fiber; scanning electron microscopy (SEM); Fourier transform infrared spectroscopy (FTIR); vacuum-assisted resin transfer molding (VARTM)

INTRODUCTION

Fiber-reinforced polymer composites have been widely utilized in structural applications because of their high specific strength, specific stiffness, corrosion resistance, fatigue resistance, and low thermal expansion relative to conventional metallic materials. However, one of the major drawbacks of composite materials is the poor interfacial adhesion between the fiber and the matrix.[1,2] The properties of composites are critically based on the microstructure and performance of an interphase between a reinforcing fiber and matrix. The ''interphase'' is a region where the fiber and matrix phases are chemically or mechanically combined.[3–6] Good adhesion is achieved almost exclusively by surface treatment through the covalent bonding of the matrix and the fiber.[7–9] Interphase between the fiber and matrix material plays an important role in binding, thus analyzing FTIR and SEM measurements of produced composites.

The surface can be analyzed by various techniques including infrared spectroscopy, FTIR, and secondary ion mass spectroscopy.[9] It is proved that FTIR spectroscopy supplies valuable information about the chemical composition of the fiber surface.[10] From the SEM study some information may be inferred about strength of fiber-matrix interactions and fiber surfaces. Extensive interfacial failure or interfacial adhesion can also be seen by using SEM analysis. Additionally, adhesive failure in the interface between carbon fiber and polyester matrix can be proved by SEM analysis.

Many industries use laminated composites, consisting of a stack of fibers oriented in the same direction, in applications that exploit their high longitudinal strength when the same properties are not required in the transverse direction. One cost-effective processing technique for glass fiber-reinforced composites is vacuum-assisted resin transfer molding (VARTM).[11]

In this work, we synthesized epoxy- and polyester-based composites made with glass and carbon fiber by solution method using a VARTM process. SEM analyses of produced materials at different magnifications were conducted to take additional information to that obtained by FTIR analysis. In addition to the extensive efforts in elucidating the type of interactions that are established between polymeric matrix and fiber material, the work presented here focuses, also, on the variation in the mechanical properties of polyester-based and epoxy-based composites. Hence, axial and transverse tensile testing was conducted up to failure on specimens strengthened with glass and carbon fabrics. In this article an

Correspondence to: M. Sarikanat (mehmet.sarikanat@ege.edu.tr).

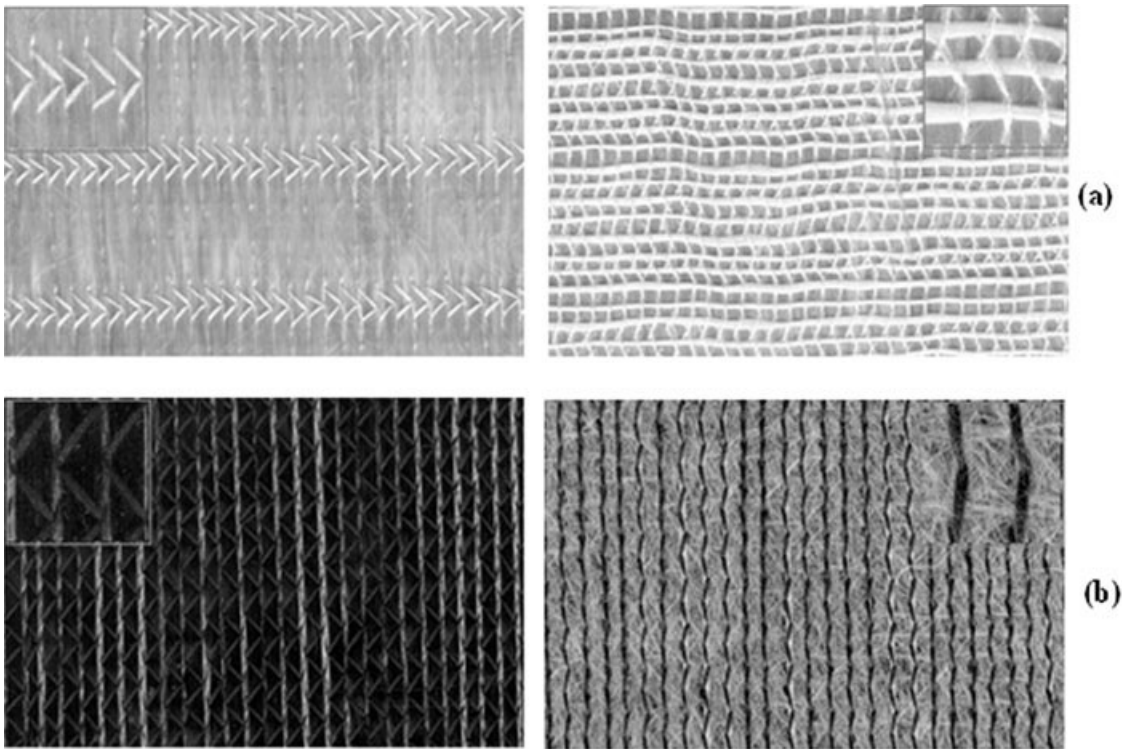

Figure 1 Sample of fabrics: (a) glass fabric; (b) carbon fabric.

important practical problem in fibrous composites, interlaminar shear strength as measured in short beam shear tests, is discussed.

EXPERIMENTAL

Materials

Glass and carbon fabric provided by Metyx Telateks Tekstil Urunleri San. Tic. A.S. (Turkey) using a Liba multiaxial warp-knitting machine was used for experimental characterization. Figure 1(a,b) show a scanned image of both sides of a piece of glass and carbon fabric, respectively. Carbon fabric is stabilized by a set of glass fibers on the bottom face [Fig. 1(b)]. Their parameters, as specified by the manufacturer, are shown in Tables I and II.

Polipol polyester 383-T resin system was used as resin in the composite. The resin, (specific gravity: 1.11 g/cm^3, viscosity brookfield: 950 Pa s), which is iso-phthalic acid type resin, was mixed before VARTM with the catalyst cobalt octoate (0.35 pph, of a 41% solution in white spirit), the retarder 2.4-pentanedione (0.10 pph), and methylethylketone peroxide (2.2 pph, of a 40% dimethyl phthalate solution). Another resin system used in this study is a two-component epoxy system from Resoltech which consists of R 1040 (unmodified liquid epoxy) and R 1048 (hardener). The composition for the epoxy resin system is specified in the product data sheet from the manufacturer is as follows (by weight): R1040 (78%) and R 1048 (22%).

Composite production

The VARTM equipment at the GOVSA Composites was used to manufacture composite plates. Composite plates having different fiber volume fractions shown in Tables III and IV (the data obtained by a resin burn-off method are the reported mean values from the manufacturer) were used for the test specimens. In the VARTM process, the entire fiber reinforced polymer composite is produced in one single operation in which resin is injected with the assistance of vacuum (Fig. 2). Fibrous preform was laid on top of the tool and was covered by a distribution medium with a high in-plane permeability to accel-

TABLE I
Specifications of Glass Fabric

Preform ID	Description	Number of plies	Total weight (g/m^2)	Plies weight (g/m^2)	Stitch pattern
GF	Glass fabric	1	472	472	Tricot

TABLE II
Specifications of Carbon Fabric

		Fibrous layers			Stitching			
Preform ID	Description	Areal density (g/m^2)	Fibre	Fibre count in tow	Stitch	Linear density (tex)	Knit pattern	Gauge (needles/inch)
CF	Carbon fabric	200	Toray T700 50E	12K	PES	5	Tricot	5

erate the in-plane flow. A plain weave nylon screen which is a type of plastic wire mesh with high porosity was used as the distribution medium. A sheet of porous peel-ply was draped over the composite to prevent the distribution medium from adhering to the cured panel and to create a clean surface. After laying up the composite panel, a spiral-wrap, 12-mm-diameter conduit was placed across the width and length of the laminate at points 2.5 cm away from the panel to ensure uniformly applied vacuum. The resin inlet was placed in the middle of the stack and was connected to a resin tank as a resin injection gate. A vacuum bag was next applied and the edges were sealed with a tacky tape. Tacky tape is a 1-in.-wide rubbery material that sticks to both the mold and the bagging material. A vacuum pump was connected to vacuum port, which was placed on glass plate, using a polyethylene tube, Figure 2.

With the vacuum bag tightly sealed and the injection gate closed, the vacuum pump was turned on. Vacuum is drawn through the vacuum line to remove air from the mold cavity, induce fiber compaction under atmospheric pressure. Then, the injection gate was opened to allow resin infusion into the high-permeable distribution medium under the atmospheric pressure. When the preform was completely infiltrated, the injection tube was clamped, and the infused panel was left to cure for 24 h at room temperature and under vacuum. After the solidified laminate was taken out of the mold, a 2-h postcure at 80°C was done in a hot press.

Fourier transform infrared spectroscopic measurements

A Fourier transform infrared (FTIR) spectrophotometer (Perkin Elmer BX-II) was employed for the entire study. One milli gram of the samples, cured resin, and fiber reinforced composites, were ground into powder with infrared-grade KBr powder (100 mg) and pressed into a pellet for measurement. Long period scanning was utilized so signal-to-noise ratio of the coadded spectrum is sufficient to resolve peaks in which we are interested. Each spectrum was recorded in the range of 400–4000 cm^{-1} with a resolution of 2 cm^{-1}. The background spectrum of KBr pellet was subtracted from the sample spectra.

Scanning electron microscopy observation

The fracture surfaces of tensile-tested specimens were examined using the scanning electron microscope (SEM; JEOL JSM 6060) at excitation voltage equal to 20 keV in the secondary electron mode. To reduce the extent of sample arcing, the samples were coated with a thin layer of metallic gold in an automatic sputter coater (Polaran SC7620) prior to examination by SEM. The sputter coater uses argon gas and a small electric field.

Tensile strength testing

The tensile experiments were conducted by longitudinal tension (ASTM D 3039) on a Shimadzu AUTOGRAPH AG-G Series universal testing machine with a video extensometer system (SHIMADZU noncontact video extensometer DVE-101/201), with Trapezium (advanced software for materials testing) for machine control and data acquisition. Tensile tests were performed at a constant cross-head speed of 2 mm/min at room temperature under air. Six tests were made for each material.

Short beam shear test

A sliding roller three-point bending fixture, which included a loading pin (diameter, 6.4 mm) and two

TABLE III
Compositions of Polyester Composites Reinforced with Glass and Carbon Fabric

Composite	Fiber volume fraction, V_f (%)	Number of fabric layers	Laminate thickness (mm)
Glass fabric	48.4 ± 0.8	12	4.8 ± 0.02
Carbon fabric	23.1 ± 1.1	12	5.78 ± 0.02

The values after the (±) refer the standard uncertainty of the measurement.

TABLE IV
Compositions of Epoxy Composites Reinforced with Glass and Carbon Fabric

Composite	Fiber volume fraction V_f (%)	Number of fabric layers	Laminate thickness (mm)
Glass fabric	33.7 ± 1.3	12	7.01 ± 0.04
Carbon fabric	24.8 ± 0.6	12	5.47 ± 0.02

The values after the (±) refer the standard uncertainty of the measurement.

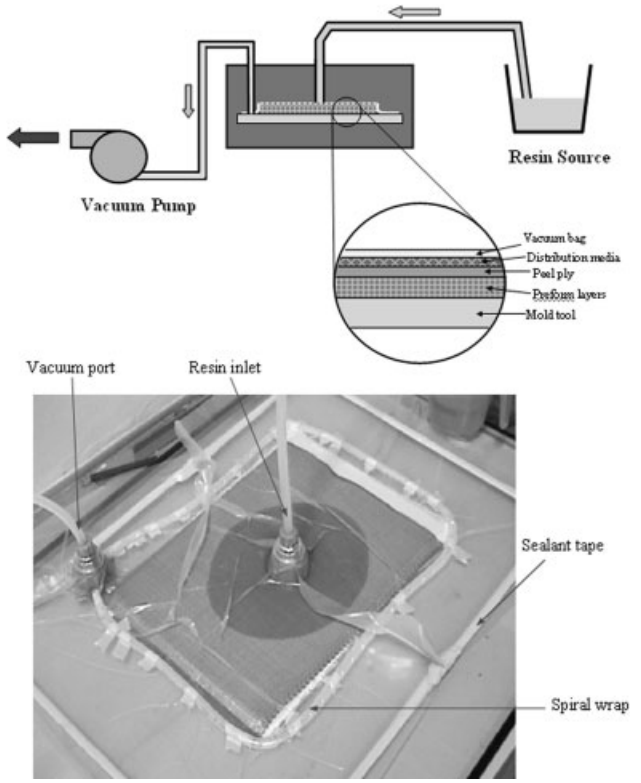

Figure 2 Vacuum-assisted resin transfer molding process and fabrication setup.

support pins (diameter, 3.2 mm), was used for the room temperature short beam shear tests. The test fixture was mounted in a 5-kN capacity, screw-driven load frame. The apparent interlaminar shear strength of composites was determined from samples that were tested with a support span/sample thickness ratio of 5 : 1. The simply supported specimens allow lateral motion and a line load is applied at the mid span of the specimens. The apparent shear strength was then calculated as follows:

$$V = 0.75\left(\frac{P_{\max}}{wt}\right) \quad (1)$$

where V is the apparent shear strength, $P_{\max}$ is the failure load, and w and t are the width and thickness of the specimen, respectively. Further details of the test procedures are given in the ASTM 2344.

RESULTS AND DISCUSSION

FTIR analysis of polyester-based composites

FTIR spectra of cured polyester, carbon fiber/polyester, and glass fiber/polyester composites were shown in Figure 3(a). The frequencies and assignments of FTIR absorption bands were summarized in Table V. The band at 3448 cm^{-1} is related to stretching vibrations of O—H groups. As can be

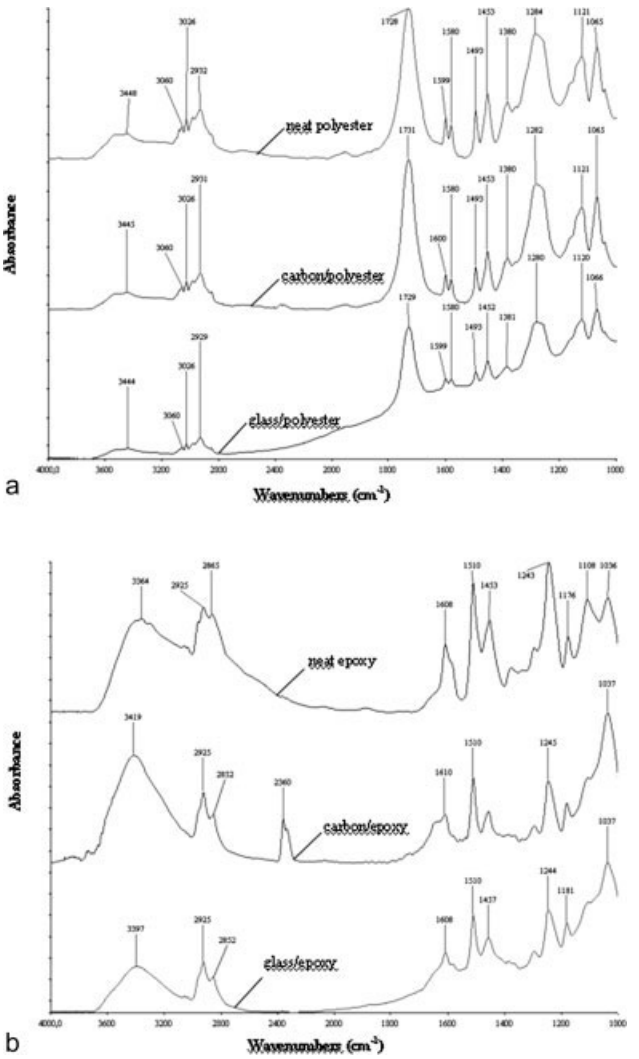

Figure 3 FTIR spectra of (a) the neat polyester resin and its glass and carbon fiber composites; (b) the neat epoxy resin and its glass and carbon fiber composites.

seen from the spectra of carbon/polyester and glass/polyester, the stretching vibrations of OH group was shifted to 3444 and 3445 cm^{-1} for glass/

TABLE V
Assignment of the Main Infrared Absorption of the Cured Neat Polyester Resin Used in This Study

Band (cm^{-1})	Assignment
3448	O—H stretch
3060	Aliphatic C—H stretch
3026	
2982	
1728	C=O stretch
1599	Aromatic ring stretch
1580	
1493	
1453	CH_3 asymmetrical bend
1380	CH_3 symmetrical bend
1284	CH_2 twist
1121	C—O stretch

TABLE VI
Assignment of the Main Infrared Absorption of the Cured Neat Epoxy Resin Used in this Study

Band (cm^{-1})	Assignment
3364	O—H stretch
2925	Aliphatic C—H stretch
2862	Aromatic ring stretch
1608	
1510 s	
1453	CH_3 asymmetrical bend
1376	CH_3 symmetrical bend
1296 m	Epoxy ring mode: the C—C, C—O
1243 s	Ar—O—R asymmetrical bend
1176	
1108	
1036	Ar—O—R symmetrical bend
828	Aromatic ring bend out of plane
753	Monosubstituted aromatic ring stretch

polyester and carbon/polyester composites, respectively. From this point of view, it is probable that hydrogen bond may occur between polyester and fiber samples. The bands in the range 2900–3100 cm^{-1} correspond to stretching vibrations of C—H groups such as CH_2 and CH_3. It is noticed that the stretching vibrations of C—H groups have approximately the same absorption bands after curing the polyester with glass and carbon fibers.

In the spectrum of cured polyester, a very intensive band was observed at 1728 cm^{-1} due to stretching vibrations of C=O group. Small changes occurs leading to the shifts of wavenumber toward higher frequencies in the spectra of glass/polyester and carbon/polyester composites. Weak bands at 1599, 1580, and 1493 cm^{-1} observed in the spectrum of cured polyester can be assigned to aromatic ring. It can be said that these bands attributed to aromatic ring do not change their positions. No interaction occurs between aromatic ring and both fibers. The bands located at 1453 and 1380 cm^{-1} may correspond to asymmetric and symmetric deformation band of methyl groups, respectively. It is seen from the spectrum of carbon/polyester composite that these bands appear simultaneously. According to Su et al.,[12] the symmetric deformation vibration of methyl groups is composed of two components, which could be assigned to the hydrated state around 1378 cm^{-1} and the other is assigned to the dehydrated state at 1373 cm^{-1}. In the current study, the symmetric C—H stretching of methyl groups located at 1380 cm^{-1} could be assigned to the hydrated state. It can be concluded that ethyl groups

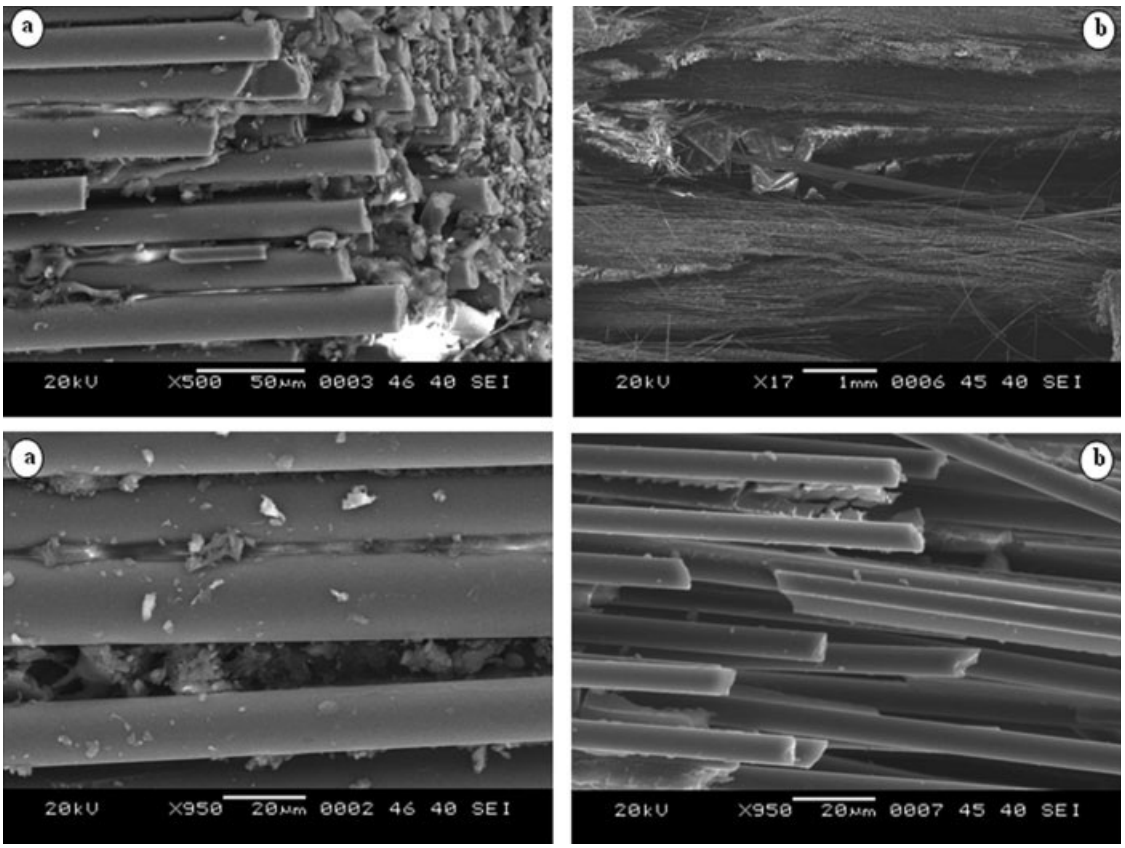

Figure 4 Representative SEM images of the breakage region for (a) glass fabric/polyester laminate and (b) carbon fabric/polyester laminate that were tensile tested in fiber direction (at different magnification levels).

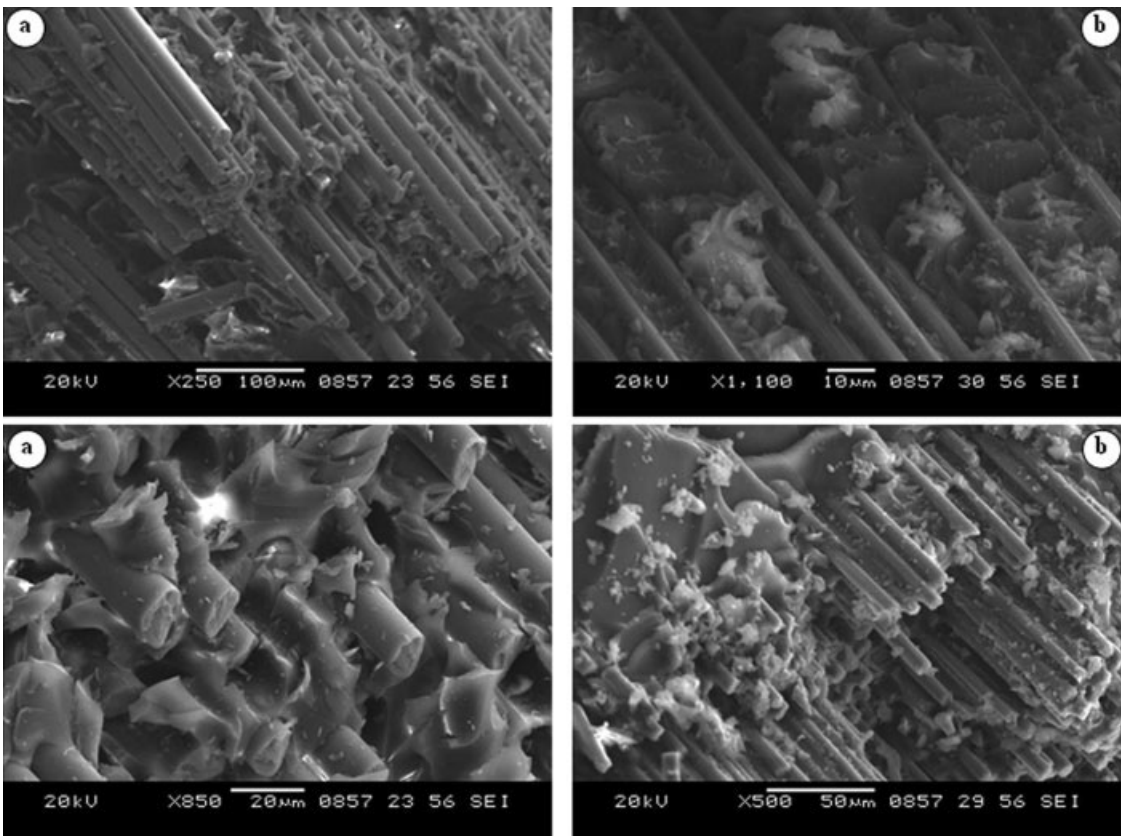

Figure 5 Representative SEM images of the breakage region for (a) glass fabric/epoxy laminate and (b) carbon fabric/epoxy laminate that were tensile tested in fiber direction (at different magnification levels).

are surrounded by water. It is probable that the microenvironment around the hydrated methyl group is polar.

The strong band at 1284 cm^{-1} which appears in the spectrum of polyester is due to twisting vibration of CH_2 groups. After the polyester resin is transferred into the fabrics and cured, the band shifted to lower frequencies. The band locations are different in the spectra of glass fiber/polyester and carbon fiber/polyester composite with a value of 1280 and 1282 cm^{-1}, respectively. It can be claimed that C—O weak interactions may occur between CH_2 groups and glass fibers. Two intensive bands at 1121 and 1065 cm^{-1} attributed to C—O stretching vibrations do not change their positions in the spectrum of carbon/polyester.

FTIR analysis of epoxy-based composites

FTIR spectra of the 100%-cured neat epoxy resin, and its carbon and glass fiber composites were shown in Figure 3(b). Table VI shows the assignment of the main infrared absorption of the neat epoxy used in this work. OH stretching vibrations of epoxy give a typical broad band at 3364 cm^{-1}. As can be seen from the spectra of the neat epoxy and its carbon and glass fiber composites, the stretching vibrations of OH groups of the epoxy resin was shifted to 3397 and 3419 cm^{-1} for glass and carbon fiber reinforced epoxy, respectively. The change in carbon/epoxy composite is higher than that of glass/epoxy composite. There is an interaction between OH groups of the epoxy resin and carbon fiber. Aliphatic C—H stretching vibrations can be seen in the range of 3000–2800 cm^{-1}. There are not so much variations for these bands.

The band at 2360 cm^{-1} in the spectrum of carbon/epoxy composite cannot be seen properly in the spectra of the neat epoxy resin and glass fiber reinforced epoxy. A new absorbing peak at 2360 cm^{-1} is observed in the spectrum of carbon/epoxy composite shows a bond formation between carbon fiber and epoxy resin. It indicates that epoxy resin has reacted with carbon fiber. It is probable that a strong interaction between carbon fiber and epoxy resin occurs in comparison with epoxy resin and glass fiber. Considering epoxide and hydroxyl group are the only two reaction groups in epoxy molecule, the 2360 cm^{-1} band may be a conclusion of bond formed by the interaction OH groups and carbon fiber.

TABLE VII
Mechanical Properties of Carbon Fiber/Polyester Composites in Different Directions

Composite	Test direction	Fiber volume fraction, V_f (%)	Tensile modulus (GPa)	Tensile strength (MPa)	Elongation at break (%)	Flexure modulus (GPa)	Flexure strength (MPa)	ILSS (MPa)
Carbon/polyester	Axial	23.1 ± 1.1	71.345 ± 2.6	641.07 ± 14.1	0.866 ± 0.04	50.445 ± 1.3	542.27 ± 12.8	21.545 ± 0.73
	Transverse		4.5440 ± 0.3	9.8980 ± 0.5	0.203 ± 0.03	4.3770 ± 0.3	22.068 ± 0.76	2.1940 ± 0.1
Glass/polyester	Axial	44.5 ± 1.8	37.827 ± 1.20	610.21 ± 14.1	1.6650 ± 0.06	27.324 ± 0.76	550.36 ± 12.8	31.218 ± 1.05
	Transverse		6.6610 ± 0.50	73.658 ± 2.85	2.2570 ± 0.10	6.6940 ± 0.32	86.477 ± 3.01	6.7510 ± 0.40
Carbon/epoxy	Axial	24.8 ± 0.6	85.706 ± 8.62	488.53 ± 14.1	0.6293 ± 0.026	25.822 ± 0.72	310.63 ± 12.54	33.765 ± 0.26
	Transverse		5.5478 ± 0.10	12.527 ± 0.163	0.2047 ± 0.011	2.1810 ± 0.023	28.251 ± 0.96	6.3288 ± 0.04
Glass/epoxy	Axial	33.7 ± 1.3	24.170 ± 3.87	399.96 ± 13.6	1.6642 ± 0.038	19.406 ± 0.36	449.75 ± 13.8	26.068 ± 0.79
	Transverse		7.2940 ± 0.16	56.636 ± 2.93	0.7655 ± 0.021	5.0025 ± 0.10	92.575 ± 6.88	10.003 ± 0.14

The data quoted are all average results taken from a minimum of six tests.
The values after the (±) refer the standard uncertainty of the measurement.

Morphological analysis of polyester-based composites

Extensive damage was found in the glass fabric laminate specimens which has poor fiber/matrix adhesion [Fig. 4(a)]. The clean fiber surfaces indicate extensive interfacial failure. In addition, there is little matrix material between the fibers on the postfracture surface, i.e., the fibers are loosely held by the matrix material. Because of the weak fiber/matrix adhesion, the damage evolution occurs at early stages of loading, and the stress transfer from critically stressed fibers to lower-stressed regions cannot be done properly. Fiber surfaces are almost completely devoid of matrix material, designating extensive interfacial failure. In addition, the matrix is no longer holding fibers together. These results may suggest that debonding between fibers and matrix or, in other words, fracture occurring in the interface between fiber and matrix because of poor interfacial adhesion could be the dominant mechanism of failure for this loading mode.

It is possible to observe clear local differences in the representative images of the breakage region for carbon fabric specimens [Fig. 4(b)]. In the upper inset, a general view is presented showing ductile deformation of the matrix but a poor matrix-carbon fiber adhesion. In the lower photomicrograph, a higher magnification image clearly shows a clean fiber surface, although a small amount of polymer can be seen between fibers. Pullout effect of fibers was observed from these images. Additionally, chemical breakage takes place in the matrix material. These observations may suggest an adhesive failure in the interface between carbon fiber and polyester matrix.

Morphological analysis of epoxy-based composites

The fracture surface of composite having glass fiber with intermediate bond strength is shown in Figure 5(a). Noncoupled composite showed uncoated fiber ends pulled from the polymer. Note the considerable amount of fiber pull-out and the irregular fracture surfaces [Fig. 5(a)]. The clean fiber surfaces on debonding cracks indicate extensive interfacial failure. Despite this fact, the fiber show traces of matrix still into and around the fiber. The fibers are loosely held by the matrix material after failure.

In plies of carbon fabric laminate [Fig. 5(b)], failure occurred by both cohesive fracture of the matrix and fiber breakage. However, composite showed considerable matrix failure together with the fibers being tightly held by the matrix material. Considerable amount of matrix tearing propagated along the resin rich region could be observed, together with cavities left by the pull-out fibers [Fig. 5(b)]. In this case, the broken matrix pieces still adhered to fibers. It can be inferred that me-

TABLE VIII
Influence of Matrix on Composite Properties

Material	TEST direction	Normalized tensile strength (MPa)	Normalized ILSS (MPa)	Average fiber content, V_f (%)
Glass/polyester	Machine	504.31	25.800	40
	Cross	60.874		
Glass/epoxy	Machine	474.73	30.941	40
	Cross	67.224		
Carbon/polyester	Machine	666.05	22.384	24
	Cross	10.285		
Carbon/epoxy	Machine	472.77	32.666	24

chanical interlocking and friction are responsible for the failure mode observed on the matrix.

Experimental results and discussions on the mechanical properties

The mechanical properties of the composites determined experimentally in different directions are shown in Table VII. To compare the mechanical properties of vacuum-infused composites reinforced with glass and carbon fabrics, the test results were normalized to the average content of fiber in the tested samples (Table VIII).

The values of matrix-dominated properties (transverse tensile strength and interlaminar shear strength) are reasonable in light of experimental work indicating that the aforementioned properties of epoxy-based composites were much better to those exhibited by polyester-based composites (Table VIII). However, an interesting but surprising observation was recorded in the longitudinal strength values of the well-bonded epoxy-based composites. For these epoxy-based composites, considerably poor performance was shown in longitudinal strengths. Contrary to epoxy-based composites, although the matrix-dominated properties were poor the longitudinal strength of polyester-based composites was much better.

A reasonable conclusion appears to be that, effectiveness of the bond between resin and fiber will not produce a high-strength composite when measured parallel to the direction of the fibers, which agrees with the conclusion drawn by Murdie et al.[13]

As can be seen from interlaminar shear strength (ILSS) results (Table VIII), the greatest ILSS value belongs to carbon/epoxy composite, when compared with that of the other composites. From the standpoint of the results of FTIR, it was claimed that a strong interaction between carbon fiber and epoxy resin occurs in comparison with epoxy resin reinforced with glass fiber. Presumably, FTIR analyses of the composites may reveal the reason why ILSS result of carbon/epoxy composite is greater than that of other composite.

CONCLUSIONS

Polyester- and epoxy-based composites containing carbon and glass fibers were fabricated using VARTM process. From the standpoint of the results of FTIR, it was claimed that a strong interaction between carbon fiber and epoxy resin occurs in comparison with epoxy resin reinforced with glass fiber. Besides, weak interactions occur between polyester and both fibers used in this work. From the morphological analysis it has been reached that micrographs suggests an adhesive failure in the interface between both fibers and polyester matrix. In the case of morphological analysis of epoxy-based composite reinforced with glass fiber, extensive interfacial failure is observed. This means that fibers are loosely held by the matrix material after failure. On the other hand, epoxy-based composite reinforced with carbon fiber showed considerable matrix failure together with the fibers. This result implies that fibers are tightly held by the matrix material. From this point of view, FTIR analysis provided good agreement with the SEM results. According to these results, among the fibers and matrix materials used in this study, carbon fiber and epoxy resin can be considered much more compatible one than the others for the production of polymer composites.

References

1. Piggott, M. R. Composites Sci Technol 1997, 57, 853.
2. Gillespie, J. W.; Mertz, D. R.; Edberg, W. M.; Ammar, N.; Kasai, K.; Hodgson, I. C. Proc Int SAMPE Tech Conf 1996, 28, 1249.
3. Tang, L. G.; Kardos, J. L. Polym Compos 1997, 18, 100.
4. Subramanian, R. V.; Jukubowski, J. J Polym Eng Sci 1978, 18, 590.
5. Zou, L. M.; Baillie, C.; Mai, Y.-W. Mater Sci 1992, 27, 3143.
6. Hoecker, F.; Karger-Kocsis J. J Appl Polym Sci 1996, 59, 139.
7. Plueddemann, E. P. Silane Coupling Agents; Plenum: New York, 1982.
8. Tang, L. G.; Kardos, J. L. Polym Compos 1997, 18, 100.
9. Danyadi, L.; Szazdi, L.; Gulyas, J.; Bertoti I.; Pukanszky, B. Compos Interfaces 2005, 12, 243.
10. Gulyás, J.; Földes, E.; Lázár, A.; Pukánszky, B. Compos A 2001, 32, 353.
11. Lee, L. Y.; Lee J. H.; Hong, C. E.; Yoo, G. H.; Advani S. G. Compos Sci Technol 2006, 66, 2116.
12. Su, Y.; Jing, W.; Liu, H. Langmuir 2002, 18, 5370.
13. Murdie, N.; Ju, C. P.; Don, J.; Wright, M. A. In Carbon-Carbon Materials and Composites; Buckley J. D.; Edie D. D., Eds.; Noyes Publications: New Jersey, 1993; Chapter 5.